Neck Rupture and Scission Neutrons in Nuclear Fission

Ibrahim Abdurrahman,[1] Matthew Kafker,[2] Aurel Bulgac,[2] and Ionel Stetcu[1]
[1]Theoretical Division, Los Alamos National Laboratory, Los Alamos, New Mexico 87545, USA
[2]Department of Physics, University of Washington, Seattle, Washington 98195–1560, USA

(Received 7 September 2023; revised 22 November 2023; accepted 30 April 2024; published 12 June 2024)

Just before a nucleus undergoes fission, a neck is formed between the emerging fission fragments. It is widely accepted that this neck undergoes a rather violent rupture, despite the absence of unambiguous experimental evidence. The main difficulty in addressing the neck rupture and saddle-to-scission stages of fission is that both are highly nonequilibrium processes. Here, we present the first fully microscopic characterization of the scission mechanism, along with the spectrum and the spatial distribution of scission neutrons (SNs), and some upper limit estimates for the emission of charged particles. The spectrum of SNs has a distinct angular distribution, with neutrons emitted in roughly equal numbers in the equatorial plane and along the fission axis. They carry an average energy around 3 ± 0.5 MeV for the fission of ^{236}U, ^{240}Pu, and ^{252}Cf, and a maximum of 16–18 MeV. We estimate a conservative lower bound of 9%–14% of the total emitted neutrons are produced at scission.

DOI: 10.1103/PhysRevLett.132.242501

Nuclear fission was experimentally discovered by Hahn and Strassmann [1] in 1939. Later in 1939, it was named and its main mechanism was explained by Meitner and Frisch [2]. It is a quantum many-body process of extreme complexity, with various parts of the process occurring at vastly different timescales. The total time it takes, from the moment a neutron initiates the formation of a compound nucleus until all final fission products have attained their equilibrium state after β decay, can be on the order of billions of years [3], and is greater by enormous orders of magnitude relative to the time it takes a nucleon to cross a nucleus, $\mathcal{O}(10^{-22})$ sec.

The compound system, formed by a low-energy neutron [1] interacting with a target nucleus, evolves through many distinct stages. The first stage is a relatively slow quasiequilibrium evolution, that lasts until the compound system [4] reaches the outer saddle point at $\approx 10^{-14}$ sec [3]. During this stage, the nucleus, with an initial prolate intrinsic shape and axial symmetry, evolves into a nucleus with triaxial shape, and eventually into a reflection asymmetric and axially symmetric elongated shape near the outer fission barrier [5]. The second stage is a highly nonequilibrium evolution from saddle to scission [6–8], when the primordial fission fragments' (FFs) properties are defined within a duration of $\approx 5 \times 10^{-21}$ sec [3]. Even though this second stage is much faster than the first stage, it corresponds to rather slow dynamics, relative to the third stage (scission). In this stage, the compound nucleus undergoes a relatively rapid separation into two FFs, lasting $\approx 10^{-22}$ sec. This stage is also known in the literature as the neck rupture. This is followed by a fourth stage, the FFs' Coulomb acceleration during an interval of time of $\mathcal{O}(10^{-18})$ sec, when at the end the FFs achieve a shape equilibration. While the initial compound nucleus is a relatively cold system with a very small spin, the primordial FFs are very hot and have relatively large spins as well [7,9]. These highly excited FFs emit prompt neutrons for an interval of time up to about $\mathcal{O}(10^{-14})$ sec, followed by the emission of the majority of prompt γ rays for an interval of time until about $\mathcal{O}(10^{-3})$ sec, which is further followed by much slower β decays. Other processes are also possible, such as delayed neutron or γ emission after β decay.

With the exception of the saddle-to-scission configuration and the neck rupture, all the other stages of fission are relatively slow quasiequilibrium processes. The fission dynamics after the compound nucleus reaches the outer saddle point has been typically described in terms of the potential energy surface of the nucleus, determined by its shape [3,10–12], not compatible with recent microscopic studies [6–8,13], and agreement with experimental data typically requires adjustment of many parameters [14]. On the other hand, many different approaches to FF mass and charge distributions lead to agreement with experiment [14–19], even though they rely on clearly contradicting physics assumptions, which simply demonstrates that these distributions are not very sensitive measures of the fission dynamics. Approximately at the top of the outer saddle, the nucleus starts forming a barely seen "wrinkle," where eventually the neck between the two FFs is formed. This wrinkle tends to appear when the fissioning nucleus is at a very early stage during the descent to scission, and its position hardly changes in time. A significant change in this position would require a large amount of energy for displacement that would not be

available from fluctuations [20–24]. At the top of the outer saddle the nucleus starts a relatively slow dissipative evolution towards scission [6–8]. During this period, the fissioning nucleus gets more elongated and the neck becomes more and more pronounced. The nuclear fluid behaves as nuclear molasses, with a very small collective velocity [6–8], while at the same time the intrinsic temperature of the system gradually increases. The bond between the two fission partners slowly weakens until the neck, which was still keeping them together, reaches a critical small diameter of approximately 3 fm and ruptures, exactly where the initial wrinkle formed much earlier at the top of the outer saddle. This dramatic separation of the two emerging FFs is a rather short-time event. For Brosa *et al.* [25] scission was the defining stage of fission, where the total kinetic energy (TKE) of the FFs is defined along with the average FF properties. The Brosa model assumes that the nucleus is a very viscous fluid, with a long neck that ruptures at a random position, and is widely invoked today in many phenomenological models [26–33], even though it has no microscopic justification and its claimed grounding in experimental data does not necessarily support a unique interpretation. Additionally, the Brosa random neck rupture model contradicts the theoretical assumptions of other popular approaches, such as the scission-point model of Wilkins *et al.* [34], where the FF formation is based on statistical equilibrium [35,36], and Brownian motion or Langevin models [14,17,37–39]. The drama of scission is followed by unavoidable debris characteristic of such dramatic separations, the scission neutrons (SNs), envisioned as early as 1939 by Bohr and Wheeler [40]. Potentially other heavier fragments, usually termed as ternary fission products [41–43], are created as well. We relegate a brief review of the history of SNs as online Supplemental Material [44], with additional references [41,42,45–88], where we also present many more details of our study.

In these simulations, we started by placing the initial compound nucleus near the top of the outer barrier in a very large simulation volume, in order to allow the emitted nucleons enough time to decouple from the FFs after the neck rupture. We have performed a range of simulations for $^{235}\mathrm{U}(\mathrm{n}_{th},\mathrm{f})$, $^{239}\mathrm{Pu}(\mathrm{n}_{th},\mathrm{f})$, and $^{252}\mathrm{Cf}(\mathrm{sf})$, using the nuclear energy density functional (NEDF) SeaLL1 [89] in simulation volumes $48^2 \times 120$ and $48^2 \times 100$ fm^3, with a lattice constant of 1 fm, for further technical details see Ref. [90]. The SeaLL1 NEDF is defined by only eight basic nuclear parameters, each related to specific nuclear properties known for decades, and contains the smallest number of phenomenological parameters of any NEDF to date [89,91]. We started the simulations at various deformations Q_{20} and Q_{30}, as listed in Ref. [44], near the outer fission barrier rim; and see Refs. [6–8], where one can find more details about how the FF properties vary with the choice of initial conditions. Our simulation volume of $48^2 \times 120$ fm^3 required the use of the entire supercomputer Summit (27 648 GPUs), corresponding to 442 TBs of total GPU memory, with further details provided in Ref. [44]. Despite this, we still could not follow the emission of nucleons for a long time, since the emitted nucleons are reflected back at the boundary relatively rapidly, see the lowest two rows of Fig. 1, where interference patterns emerge. In the transversal direction the reflection from the boundaries occurs earlier than along the fission axis, and that has affected some of the properties of the nucleons emitted perpendicular to the fission axis. However, the effect is minor, see Ref. [44].

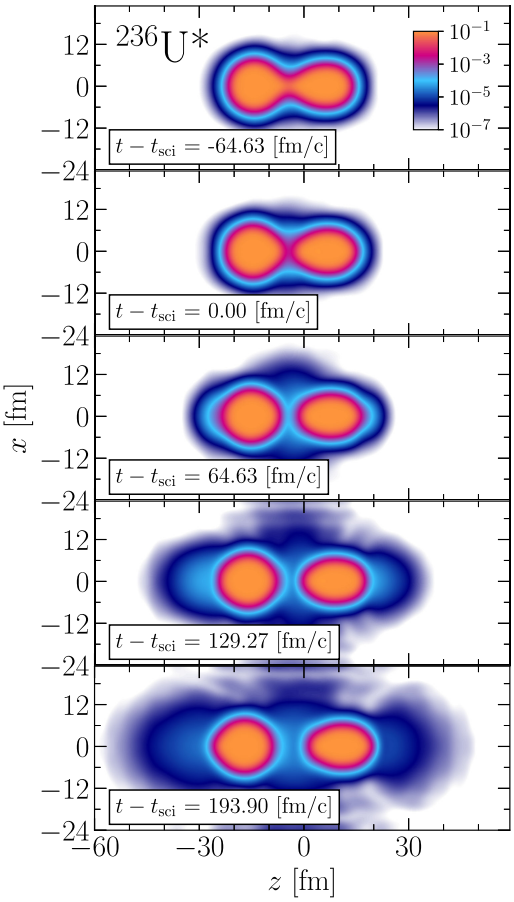

FIG. 1. Time series of the neutron number density in fm^{-3} for a typical fission trajectory. Similar results for protons are contained in the Supplemental Material [44].

From here, we will concentrate on the dynamics of the neck formation and rupture, followed by the emission of nucleons, all treated within the time-dependent density functional theory extended to superfluid fermionic systems [92]. The integrated neck density, shown in Fig. 2, is defined as

$$n_{\mathrm{neck},\tau}(t) = \int dxdy\, n_\tau(x, y, z_{\mathrm{neck}}, t), \qquad \tau = n, p, \qquad (1)$$

separately for neutrons and protons, where the $z_{\rm neck}$ is the position along the fission axis Oz where the neck has the smallest radius. The neck decays relatively slowly at scission, until its diameter reaches about 3 fm, after which it undergoes a very rapid decay. Different curves illustrated in the lower panel correspond to trajectories started at various initial conditions for the deformations Q_{20}, Q_{30} close to the outer fission barrier [44]. The time to reach scission can vary significantly, depending on the initial values of the deformations Q_{20}, Q_{30} and on the NEDF used, typically ranging from 1,000 to 3,000 fm/c.

These microscopic results illustrate several points, which were unknown until now, due to the absence of any detailed fully microscopic quantum many-body simulations of fission dynamics. First, the wrinkle in the nuclear density, where the neck is eventually formed and where the nucleus eventually scissions, is determined a long time before the nucleus reaches scission. Within the time-dependent density functional theory (TDDFT) framework the position of the neck rupture is not random, unlike in the Brosa model [25,44]. At the time when the neck reaches a critical diameter of ≈3 fm, the nuclear surface tension and the shape of the compound around the neck region, can no longer counteract the strong Coulomb repulsion between the preformed FFs, causing the system to violently "snap." One should keep in mind that as the intrinsic temperature of the compound nucleus increases, the surface tension also decreases. The geometry of the nuclear shape changes dramatically at this stage, from exhibiting a neck region where the Gaussian curvature is negative, to two separated FFs with surfaces characterized by predominantly positive Gaussian curvatures.

Second, the proton neck completes its rupture earlier than the neutron neck does, see lower panel in Fig. 2, resulting in the neck being mostly sustained by the neutrons just before the full rupture. This is similar to the neutron density in the neutron skin of heavy nuclei. In this time interval, the number of neutrons per unit area at the neck varies by an order of magnitude. The protons in the emerging FFs separate about 50–100 fm/c before the neutron's neck ruptures. Additionally, the integrated neutron and proton densities at $z_{\rm neck}$ asymptotically reach almost equilibrium values, after the neck ruptures.

Third, the rupture is unarguably the fastest stage of the fission dynamics, starting from the capture of the incident neutron and formation of the compound nucleus, until all fission products have been emitted. The decay times are 15 fm/c and 35 fm/c for proton and neutron necks, respectively, which are significantly faster processes than the time it takes the fastest nucleon to communicate any information or facilitate any kind of equilibrium between the two preformed FFs, which is at minimum ∼160 fm/c.

Fourth, the neck decay dynamics displays a clear universality (for asymmetric fission) irrespective of the initial conditions, as shown in the lower panel of Fig. 2,

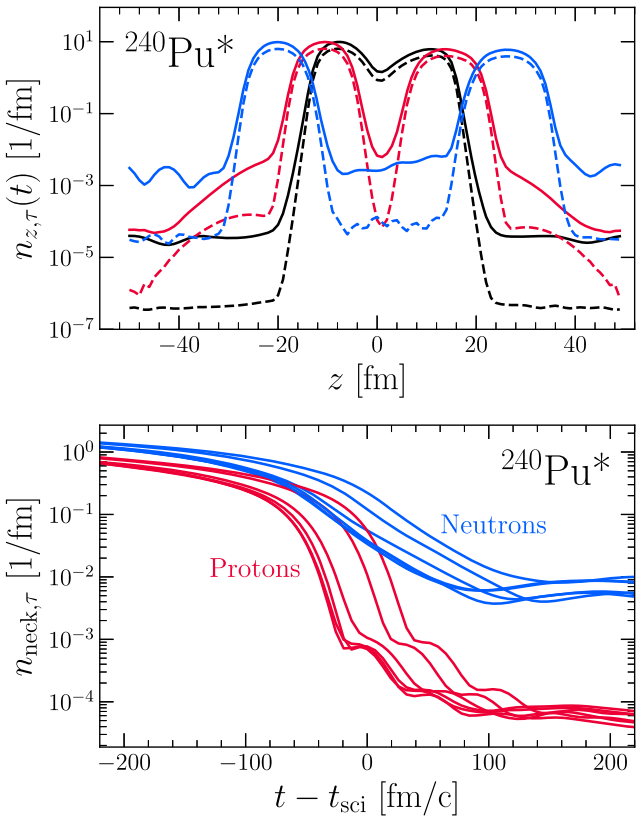

FIG. 2. In the upper panel we display the integrated nucleon density along the fission axis $n_{z,\tau}(t) = \int dxdy\, n_\tau(x, y, z, t)$ at several times; before scission at −258.53 fm/c (black lines), when the neck is barely formed; after scission at 129.27 fm/c (red lines); and after the FFs separated, respectively, at 517.06 fm/c (blue lines). Neutrons (protons) are represented via solid (dashed) lines, respectively. In the bottom panel, the nucleon number density integrated over the cross section of the neck as a function of time. A fit around the scission time, shows that integrated over the cross section of the neck, the neutron number density decays exponentially, $n_{{\rm neck},\tau}(t) \sim \exp(-t/\tau)$, with $\tau \approx 35.0 \pm 2.2$ fm/c for neutrons and 15.3 ± 0.3 fm/c for protons.

with the proton neck rupturing well ahead of the neutron neck, due to the presence of a well-defined neutron skin. The proton and neutron neck ruptures are the same for all trajectories, unlike any other outcomes of the fission process [7,8].

Last, the scission mechanism emerging from a fully microscopic treatment of the fission dynamics is totally at odds with previous models, including the Brosa random rupture model and the scission-point models. TDDFT extended to superfluid systems is the only theoretical microscopic framework so far in the literature in which scission is treated without any unchecked assumptions or fitting parameters, which produces results that are in agreement with data [6–8,92].

The neck rupture is a very fast "healing" process of the nuclear surface in the neck region. Unlike a gas in a

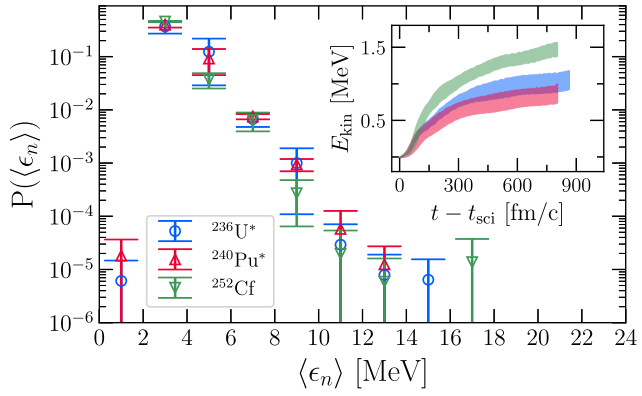

FIG. 3. The scission neutron kinetic energy distribution with uncertainties corresponding to different trajectories. The distributions are normalized to the total number of SNs, i.e., $\sum \mathrm{P}(\langle\epsilon_n\rangle) \times (\Delta E/\mathrm{MeV}) = N_{\mathrm{sci}}$, with $\Delta E = 2$ MeV. The inset shows the total kinetic energy of the SNs vs time. The shaded regions represent the standard deviation from considering various trajectories.

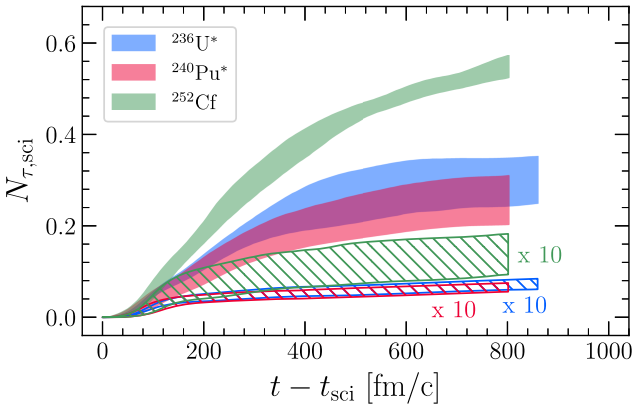

FIG. 4. The solid (dashed) regions show the number of SNs (protons), respectively; $\tau = n, p$. The shaded regions represent the standard deviation from considering various trajectories. $N_{p,\mathrm{sci}}$ was enhanced by a factor of 10.

punctured balloon, which would rapidly escape the enclosure, due to the presence of the nuclear "skin" and strong surface tension, the nucleus behaves as a fluid. The surface tension quickly "heals" the "wound," however, a small fraction of matter manages to escape like a gas, with no droplet formation, see Fig. 1. The potential condensation of this emitted gas into light charged particles cannot be described within the present framework, which includes at most two particle correlations. This is not to be confused with ternary fission of a preformed fragment, where further discussion is provided in Ref. [44]. In Fig. 1, and more in Ref. [44], we show several representative frames for neutrons and protons of the neck formation and emission of nucleons.

The most remarkable features of this process are the following. As visible in Fig. 2, the proton neck completes its rupture before the neutron neck, however, in two stages. Immediately at scission, which in Fig. 1 is identified with the rupture of the proton neck, a number of nucleons are emitted in the plane perpendicular to the fission axis (see second time frame). After a sufficient time for nucleons to propagate from the neck to the nose of each FF, scission nucleons also appear propagating in front of each FF. In 1984, it was suggested by Mädler [93], that the reabsorption of the neck stumps by the FFs, being a relatively rapid process, could act as a "catapult," which is more appropriately described as a slingshot, and "push" nucleons out of the front of the FFs. It is also important to note, the formation of three neutron clouds, two in front of the FFs and one transverse ring perpendicular to the fission axis, appears across all considered trajectories and nuclei thus far.

Remembering that the TKE is roughly 171–186 MeV, at the end of the full Coulomb acceleration the light and heavy FFs will have an average kinetic energy per nucleon of about 1 MeV and 0.5 MeV, respectively, which is significantly lower than the average kinetic energy of the SNs, see Fig. 3, given by 3.51 ± 0.25 MeV, 3.42 ± 0.27 MeV, and 2.67 ± 0.24 MeV for ^{236}U, ^{240}Pu, and ^{252}Cf, respectively. As noted by R. Capote [94], our results, which are consistent with high-energy neutrons observed via dosimetry measurements [95], point to an unmistakable need to include SNs in the analysis of prompt neutron spectra [96]. As a result, the FFs will never have a chance to catch up with them. Additionally, the SNs are essentially free, since their total interaction energy, estimated using the neutron equation of state [89],

$$E_n^{\mathrm{int}} = \int dV \left[a_n n_n^{5/3} + b_n n_n^2 + c_n n_n^{7/3}\right] \ll E_n^{\mathrm{kin}}, \quad (2)$$

comprises less than 1% percent of their kinetic energy. The total number of emitted neutrons, shown in Fig. 4, is about 0.30 ± 0.05, 0.26 ± 0.05, and 0.55 ± 0.02 per fission event for ^{236}U, ^{240}Pu, and ^{252}Cf, respectively, which is a considerable portion (roughly 9%–14%) of the total emitted prompt neutrons, see Refs. [41,43]. These are somewhat conservative estimates, see the discussion in Ref. [44], and these numbers can be likely enhanced by at least a factor of 1.25. This is clear in Fig. 4 where neither the emission of neutrons or protons has flattened. In comparison, Carjan *et al.* [52,97–100] estimated an upper bound of 25%–50% of prompt fission neutrons are emitted during scission. At the same time the number of emitted protons is about 2 orders of magnitude lower, see Fig. 4. The nucleons are emitted in roughly equal numbers both transverse to the scission axis and in front of the FFs.

In summary, we have clarified several aspects of the most nonequilibrium and fastest stage of nuclear fission dynamics. Within TDDFT, the neck rupture is not a random process, as previously argued in various phenomenological

models. Additionally, it appears that the neck rupture has similar dynamics for a large class of asymmetric fission events, irrespective of the nucleus considered or the initial conditions, beyond the top of the outer fission barrier. This universality carries over to the emission of SNs, whose signal always appears as three distinct clouds, one transverse to the fission axis and two in front of each FF, in almost equal proportions. The aspects of the neck dynamics discussed above, can serve as a theoretical input for any semiphenomenological approach to study FF properties [27–30].

The idea of SNs, proposed by Bohr and Wheeler [40], is almost as old as nuclear fission itself. The existence of SNs has been debated over the years [45,48,52,97–118], see also *Historical Note* in Ref. [43], and their experimental confirmation is still an open question. While neutron properties in earlier studies using simplified models [52,99,100] have some features somewhat similar to what we find, they are missing the major component of emission perpendicular to the fission axis. The small fraction of SNs carry noticeable kinetic energy, and what is more surprising is that their energy spectrum ranges up to almost 18 MeV, as shown in Fig. 3, similar to other observations [94,96]. Along with SNs, a very small fraction of protons are emitted as well, and their fraction suggests a theoretical estimate for the emission of α particles and other charged nuclei.

We thank Kyle Godbey and Guillaume Scamps for many useful discussions, and Roberto Capote for his feedback regarding the impact of this work on the description of prompt fission neutron spectra. The work of I. A. and I. S. was supported by the U.S. Department of Energy through the Los Alamos National Laboratory. The Los Alamos National Laboratory is operated by Triad National Security, LLC, for the National Nuclear Security Administration of the U.S. Department of Energy Contract No. 89233218CNA000001. I. A. and I. S. gratefully acknowledge partial support and computational resources provided by the Advanced Simulation and Computing (ASC) Program. The work of M. K. and A. B. was supported by the US DOE, Office of Science, Grant No. DE-FG02-97ER41014 and also partially by NNSA cooperative Agreement DE-NA0003841, and is greatly appreciated. This research used resources of the Oak Ridge Leadership Computing Facility, which is a U.S. DOE Office of Science User Facility supported under Contract No. DE-AC05-00OR22725.

[1] O. Hahn and F. Strassmann, Über den Nachweis und das Verhalten der bei der Bestrahlung des Urans mittels Neutronen entstehenden Erdalkalimetalle, Naturwissenschaften **27**, 11 (1939).
[2] L. Meitner and O. R. Frisch, Disintegration of uranium by neutrons: A new type of nuclear reaction, Nature (London) **143**, 239 (1939).
[3] F. Gönnenwein, Neutron and gamma emission in fission, LANL Fiesta 2014 Lectures (2014).
[4] N. Bohr, Neutron capture and nuclear constitution, Nature (London) **137**, 344 (1936).
[5] W. Ryssens, P.-H. Heenen, and M. Bender, Numerical accuracy of mean-field calculations in coordinate space, Phys. Rev. C **92**, 064318 (2015).
[6] A. Bulgac, P. Magierski, K. J. Roche, and I. Stetcu, Induced fission of ^{240}Pu within a real-time microscopic framework, Phys. Rev. Lett. **116**, 122504 (2016).
[7] A. Bulgac, S. Jin, K. J. Roche, N. Schunck, and I. Stetcu, Fission dynamics of ^{240}Pu from saddle to scission and beyond, Phys. Rev. C **100**, 034615 (2019).
[8] A. Bulgac, S. Jin, and I. Stetcu, Nuclear fission dynamics: Past, present, needs, and future, Front. Phys. **8**, 63 (2020).
[9] A. Bulgac, I. Abdurrahman, S. Jin, K. Godbey, N. Schunck, and I. Stetcu, Fission fragment intrinsic spins and their correlations, Phys. Rev. Lett. **126**, 142502 (2021).
[10] P. Ring and P. Schuck, *The Nuclear Many-Body Problem*, 1st ed. (Springer-Verlag, Berlin Heidelberg, New York, 2004).
[11] J. K. Krappe and K. Pomorski, *Theory of Nuclear Fission* (Springer Heidelberg, 2012).
[12] N. Schunck and L. M. Robledo, Microscopic theory of nuclear fission: A review, Rep. Prog. Phys. **79**, 116301 (2016).
[13] M. Bender *et al.*, Future of nuclear fission theory, J. Phys. G **47**, 113002 (2020).
[14] A. J. Sierk, Langevin model of low-energy fission, Phys. Rev. C **96**, 034603 (2017).
[15] M. Verriere, N. Schunck, and D. Regnier, Microscopic calculation of fission product yields with particle-number projection, Phys. Rev. C **103**, 054602 (2021).
[16] M. R. Mumpower, P. Jaffke, M. Verriere, and J. Randrup, Primary fission fragment mass yields across the chart of nuclides, Phys. Rev. C **101**, 054607 (2020).
[17] F. A. Ivanyuk, C. Ishizuka, and S. Chiba, Five-dimensional Langevin approach to fission of atomic nuclei, Phys. Rev. C **109**, 034602 (2024).
[18] J. Sadhukhan, W. Nazarewicz, and N. Schunck, Microscopic modeling of mass and charge distributions in the spontaneous fission of ^{240}Pu, Phys. Rev. C **93**, 011304(R) (2016).
[19] J. Sadhukhan, C. Zhang, W. Nazarewicz, and N. Schunck, Formation and distribution of fragments in the spontaneous fission of ^{240}Pu, Phys. Rev. C **96**, 061301(R) (2017).
[20] D. L. Hill and J. A. Wheeler, Nuclear constitution and the interpretation of fission phenomena, Phys. Rev. **89**, 1102 (1953).
[21] J. J. Griffin and J. A. Wheeler, Collective motions in nuclei by the method of generator coordinates, Phys. Rev. **108**, 311 (1957).
[22] P. G. Reinhard, R. Y. Cusson, and K. Goeke, Time evolution of coherent ground-state correlations and the tdhf approach, Nucl. Phys. **A398**, 141 (1983).
[23] A. Bulgac, S. Jin, and I. Stetcu, Unitary evolution with fluctuations and dissipation, Phys. Rev. C **100**, 014615 (2019).
[24] A. Bulgac, Pure quantum extension of the semiclassical Boltzmann-Uehling-Uhlenbeck equation, Phys. Rev. C **105**, L021601 (2022).
[25] U. Brosa, S. Grossmann, and A. Müller, Nuclear scission, Phys. Rep. **197**, 167 (1990).

[26] S. Oberstedt, F.-J. Hambsch, and F. Vivès, Fission-mode calculations for 239U, a revision of the multi-modal random neck-rupture model, Nucl. Phys. **A644**, 289 (1998).

[27] R. Vogt, J. Randrup, J. Pruet, and W. Younes, Event-by-event study of prompt neutrons from ^{239}Pu(n,f), Phys. Rev. C **80**, 044611 (2009).

[28] B. Becker, P. Talou, T. Kawano, Y. Danon, and I. Stetcu, Monte Carlo Hauser-Feshbach predictions of prompt fission γ rays: Application to $n_{\mathrm{th}} + ^{235}$U, $n_{\mathrm{th}} + ^{239}$Pu, and ^{252}Cf (sf), Phys. Rev. C **87**, 014617 (2013).

[29] P. Talou, I. Stetcu, P. Jaffke, M. E. Rising, A. E. Lovell, and T. Kawano, Fission fragment decay simulations with the CGMF code, Comput. Phys. Commun. **269**, 108087 (2021).

[30] O. Litaize, O. Serot, D. Regnier, S. Theveny, and S. Onde, New features of the FIFRELIN code for the investigation of fission fragments characteristics, Phys. Procedia **31**, 51 (2012).

[31] A. E. Lovell, T. Kawano, S. Okumura, I. Stetcu, M. R. Mumpower, and P. Talou, Extension of the Hauser-Feshbach fission fragment decay model to multichance fission, Phys. Rev. C **103**, 014615 (2021).

[32] K. Fujio, A. Al-Adili, F. Nordström, J.-F. Lemaître, S. Okumura, S. Chiba, and A. Koning, TALYS calculations of prompt fission observables and independent fission product yields for the neutron-induced fission of ^{235}U, Eur. Phys. J. A **59**, 178 (2023).

[33] T. Najumunnisa, M. M. Musthafa, C. V. Midhun, Muhammed Aslam, K. K. Rajesh, P. Surendran, J. P. Nair, A. Shanbhag, and S. Ghugre, ^{105}Rh yield from the proton induced fission of uranium, Nucl. Phys. **A1032**, 122611 (2023).

[34] B. D. Wilkins, E. P. Steinberg, and R. R. Chasman, Scission-point model of nuclear fission based on deformed-shell effects, Phys. Rev. C **14**, 1832 (1976).

[35] J.-F. Lemaître, S. Panebianco, J.-L. Sida, S. Hilaire, and S. Heinrich, New statistical scission-point model to predict fission fragment observables, Phys. Rev. C **92**, 034617 (2015).

[36] J.-F. Lemaître, S. Goriely, A. Bauswein, and H.-T. Janka, Fission fragment distributions and their impact on the *r*-process nucleosynthesis in neutron star mergers, Phys. Rev. C **103**, 025806 (2021).

[37] J. Randrup and P. Möller, Brownian shape motion on five-dimensional potential-energy surfaces:Nuclear fission-fragment mass distributions, Phys. Rev. Lett. **106**, 132503 (2011).

[38] M. Albertsson, B. G. Carlsson, T. Døssing, P. Möller, J. Randrup, and S. Åberg, Excitation energy partition in fission, Phys. Lett. B **803**, 135276 (2020).

[39] M. Verriere and M. R. Mumpower, Improvements to the macroscopic-microscopic approach of nuclear fission, Phys. Rev. C **103**, 034617 (2021).

[40] N. Bohr and J. A. Wheeler, The mechanism of nuclear fission, Phys. Rev. **56**, 426 (1939).

[41] R. Vandenbosch and J. R. Huizenga, *Nuclear Fission* (Academic Press, New York, 1973).

[42] H. J. Rose and G. A. Jones, A new kind of natural radioactivity, Nature (London) **307**, 245 (1984).

[43] *The Nuclear Fission Process*, edited by C. Wagemans (CRC Press, Boca Raton, 1991).

[44] See Supplemental Material at http://link.aps.org/supplemental/10.1103/PhysRevLett.132.242501 for a brief overview of the history of scission neutrons, discusses charged particle emission at scission, methodology, collective flow energy, and the use of potential energy surfaces (PES) for fission calculations.

[45] S. Debenedetti, J. E. Francis, W. M. Preston, and T. W. Bonner, Angular dependence of coincidences between fission neutrons, Phys. Rev. **74**, 1645 (1948).

[46] J. S. Fraser, The angular distribution of prompt neutrons emitted in fission, Phys. Rev. **88**, 536 (1952).

[47] J. S. Fraser and J. C. D. Milton, Distribution of prompt-neutron emission probability for the fission fragments of U^{233}, Phys. Rev. **93**, 818 (1954).

[48] V. S. Stavinsky, On the emission mechanism of prompt fission neutrons, J. Exp. Theor. Phys. **9**, 437 (1959), http://jetp.ras.ru/cgi-bin/dn/e_009_02_0437.pdf.

[49] I. Halpern, Nuclear fission, Annu. Rev. Nucl. Part. Sci. **9**, 245 (1959).

[50] A. S. Vorobyev, O. A. Shcherbakov, A. M. Gagarski, G. V. Val'ski, and G. A. Petrov, Investigation of the prompt neutron emission mechanism in low energy fission of ^{235,233}U$(n_{\mathrm{th}}f)$ and ^{252}Cf(sf), EPJ Web Conf. **8**, 03004 (2010).

[51] U. Brosa and H.-H. Knitter, The scission neutron spectrum of ^{252}CF (SF), Z. Phys. A **343**, 39 (1992).

[52] M. Rizea, V. Ledoux, M. V. Daele, G. V. Berghe, and N. Carjan, Finite difference approach for the two-dimensional Schrödinger equation with application to scission-neutron emission, Comput. Phys. Commun. **179**, 466 (2008).

[53] I. Stetcu, A. Bulgac, P. Magierski, and K. J. Roche, Isovector giant dipole resonance from the 3D time-dependent density functional theory for superfluid nuclei, Phys. Rev. C **84**, 051309(R) (2011).

[54] Y. Tanimura, D. Lacroix, and S. Ayik, Microscopic phase-space exploration modeling of ^{258}Fm spontaneous fission, Phys. Rev. Lett. **118**, 152501 (2017).

[55] Z. X. Ren, D. Vretenar, T. Nikšić, P. W. Zhao, J. Zhao, and J. Meng, Dynamical synthesis of ^{4}He in the scission phase of nuclear fission, Phys. Rev. Lett. **128**, 172501 (2022).

[56] G. Scamps, D. Lacroix, G. F. Bertsch, and K. Washiyama, Pairing dynamics in particle transport, Phys. Rev. C **85**, 034328 (2012).

[57] A. Bulgac, Examining the justification for the introduction of a fermion localization function, Phys. Rev. C **108**, L051303 (2023).

[58] P. Demers, Pairs of fission fragments from U^{235}, Phys. Rev. **70**, 974 (1946).

[59] G. Farwell, E. Segrè, and C. Wiegand, Long range alpha-particles emitted in connection with fission. Preliminary report, Phys. Rev. **71**, 327 (1947).

[60] E. O. Wollan, C. D. Moak, and R. B. Sawyer, Alpha-particles associated with fission, Phys. Rev. **72**, 447 (1947).

[61] L. Marshall, Alpha-Particles from fission as recorded by photographic emulsions, Phys. Rev. **75**, 1339 (1949).

[62] W. E. Titterton, Slow-neutron ternary fission of uranium-235, Nature (London) **168**, 590 (1951).

[63] K. W. Allen and J. T. Dewan, The emission of long-range charged particles in the slow neutron fission of heavy nuclei, Phys. Rev. **80**, 181 (1950).

[64] N. Feather, Emission of secondary charged particles in fission, Nature (London) **159**, 607 (1947).

[65] R. A. Nobles, Long-range particles from nuclear fission, Phys. Rev. **126**, 1508 (1962).

[66] Z. Fraenkel, Emission of long-range alpha particles in the spontaneous fission of Cf^{252}, Phys. Rev. **156**, 1283 (1967).

[67] E. L. Albenesius, Tritium as a product of fission, Phys. Rev. Lett. **3**, 274 (1959).

[68] J. C. Watson, High-energy alpha particles and tritons from the spontaneous fission of californium-252, Phys. Rev. **121**, 230 (1961).

[69] M. Marshall and J. Scobie, The emission of alpha particles and tritons in the thermal neutron fission of ^{235}U, Phys. Lett. **23**, 583 (1966).

[70] F. K. Goward, E. W. Titterton, and J. J. Wilkins, Photo-fission of uranium with possible emission of a beryllium nucleus, Nature (London) **164**, 661 (1949).

[71] S. L. Whetstone and T. D. Thomas, Spontaneous emission of energetic He^6 particles from Cf^{252}, Phys. Rev. Lett. **15**, 298 (1965).

[72] M. Dakowski, J. Chwaszczewska, T. Krogulski, E. Piasecki, and M. Sowinski, Energy spectra of long range particles from the thermal neutron fission of ^{235}U, Phys. Lett. B **25**, 213 (1967).

[73] S. W. Cosper, J. Cerny, and R. C. Gatti, Long-range particles of $Z = 1$to4 emitted during the spontaneous fission of ^{252}Cf, Phys. Rev. **154**, 1193 (1967).

[74] T. Krogulski, J. Chwaszczewska, M. Dakowski, E. Piasecki, M. Sowiński, and J. Tys, Emission of light nuclei in thermal neutron fission of ^{239}Pu, Nucl. Phys. **A128**, 219 (1969).

[75] J. Chwaszczewska, M. Dakowski, T. Krogulski, E. Piasecki, W. Przyborski, and M. Sowiński, Emission of long-range charged particles in the fission of ^{235}U induced by thermal neutrons, Phys. Lett. B **24**, 87 (1967).

[76] A. A. Vorobiev, D. M. Seleverstov, V. T. Grachov, I. A. Kondurov, A. M. Nikitin, A. I. Yegorov, and Y. K. Zalite, Light nuclei from ^{233}U neutron fission, Phys. Lett. B **30**, 332 (1969).

[77] D. N. Poenaru, W. Greiner, K. Depta, M. Ivascu, D. Mazilu, and A. Sandulescu, Calculated half-lives and kinetic energies for spontaneous emission of heavy ions from nuclei, At. Data Nucl. Data Tables **34**, 423 (1986).

[78] F. Dalfovo, S. Giorgini, L. P. Pitaevskii, and S. Stringari, Theory of Bose-Einstein condensation in trapped gases, Rev. Mod. Phys. **71**, 463 (1999).

[79] C. J. Pethick and H. Smith, *Bose–Einstein Condensation in Dilute Gases* (Cambridge University Press, Cambridge, 2008).

[80] S. Giorgini, L. P. Pitaevskii, and S. Stringari, Theory of ultracold atomic Fermi gases, Rev. Mod. Phys. **80**, 1215 (2008).

[81] R. H. Fowler and L. Nordheim, Electron emission in intense electric fields, Proc. R. Soc. A **119**, 173 (1928).

[82] E. A. Uehling and G. E. Uhlenbeck, Transport phenomena in Einstein-Bose and Fermi-Dirac gases. I, Phys. Rev. **43**, 552 (1933).

[83] G. F. Bertsch and S. Das Gupta, A guide to microscopic models for intermediate energy heavy ion collisions, Phys. Rep. **160**, 189 (1988).

[84] A. Bulgac, M. Kafker, I. Abdurrahman, and I. Stetcu, Non-Markovian character and irreversibility of real-time quantum many-body dynamics, Phys. Rev. C **107**, L061602 (2023).

[85] J. C. Tully and R. K. Preston, Trajectory surface hopping approach to nonadiabatic molecular collisions: The reaction of H+ with D2, J. Chem. Phys. **55**, 562 (1971).

[86] J. C. Tully, Molecular dynamics with electronic transitions, J. Chem. Phys. **93**, 1061 (1990).

[87] S. Hammes-Schiffer and J. C. Tully, Proton transfer in solution: Molecular dynamics with quantum transitions, J. Chem. Phys. **101**, 4657 (1994).

[88] P. Fröbrich and I. I. Gontchar, Langevin description of fusion, deep-inelastic collisions and heavy-ion-induced fission, Phys. Rep. **292**, 131 (1998).

[89] A. Bulgac, M. M. Forbes, S. Jin, R. N. Perez, and N. Schunck, Minimal nuclear energy density functional, Phys. Rev. C **97**, 044313 (2018).

[90] S. Jin, K. J. Roche, I. Stetcu, I. Abdurrahman, and A. Bulgac, The LISE package: Solvers for static and time-dependent superfluid local density approximation equations in three dimentions, Comput. Phys. Commun. **269**, 108130 (2020).

[91] A. Bulgac, M. Kafker, and I. Abdurrahman, Measures of complexity and entanglement in many-fermion systems, Phys. Rev. C **107**, 044318 (2023).

[92] A. Bulgac, Time-dependent density functional theory for fermionic superfluids: From cold atomic gases, to nuclei and neutron star crust, Phys. Status Solidi (b) **256**, 1800592 (2019).

[93] P. Mädler, Catapult mechanism for fast particle emission in fission and heavy ion reactions, Z. Phys. A **321**, 343 (1985).

[94] R. Capote, Private communication (2023).

[95] M. Schulc, M. Kostal, R. Capote, J. Simon, T. Czakoj, and E. Novak, Spectral averaged cross sections as a probe to a high energy tail of ^{233}U PFNS, EPJ Web Conf. **284**, 04021 (2023).

[96] D. A. Brown, M. B. Chadwick, R. Capote, A. C. Kahler, A. Trkov, M. W. Herman, A. A. Sonzogni, Y. Danon, A. D. Carlson, M. Dunn *et al.*, ENDF/B-VIII. 0: The 8th major release of the nuclear reaction data library with CIELO-project cross sections, new standards and thermal scattering data, Nucl. Data Sheets **148**, 1 (2018).

[97] N. Carjan and M. Rizea, Scission neutrons and other scission properties as function of mass asymmetry in $^{235}U(n_{th}, f)$, Phys. Rev. C **82**, 014617 (2010).

[98] N. Carjan and M. Rizea, Similarities between calculated scission-neutron properties and experimental data on prompt fission neutrons, Phys. Lett. B **747**, 178 (2015).

[99] R. Capote, Y.-J. Chen, F.-J. Hambsch, N. V. Kornilov, J. P. Lestone, O. Litaize, B. Morillon, D. Neudecker, S. Oberstedt, T. Ohsawa, N. Otuka, V. G. Pronyaev,

A. Saxena, O. Serot, O. A. Shcherbakov, N.-C. Shu, D. L. Smith, P. Talou, A. Trkov, A. C. Tudora, R. Vogt, and A. S. Vorobyev, Prompt fission neutron spectra of actinides, Nucl. Data Sheets **131**, 1 (2016), special Issue on Nuclear Reaction Data.

[100] N. Carjan and M. Rizea, Structures in the energy distribution of the scission neutrons: Finite neutron-number effect, Phys. Rev. C **99**, 034613 (2019).

[101] R. R. Wilson, Directional properties of fission neutrons, Phys. Rev. **72**, 189 (1947).

[102] R. W. Fuller, Dependence of neutron production in fission on rate of change of nuclear potential, Phys. Rev. **126**, 684 (1962).

[103] H. R. Bowman, S. G. Thompson, J. C. D. Milton, and W. J. Swiatecki, Velocity and angular distributions of prompt neutrons from spontaneous fission of Cf^{252}, Phys. Rev. **126**, 2120 (1962).

[104] S. S. Kapoor, R. Ramanna, and P. N. Rama Rao, Emission of prompt neutrons in the thermal neutron fission of U^{235}, Phys. Rev. **131**, 283 (1963).

[105] K. Skarsvåg and K. Bergheim, Energy and angular distributions of prompt neutrons from slow neutron fission of U^{235}, Nucl. Phys. **45**, 72 (1963).

[106] A. Gavron and Z. Fraenkel, Neutron correlations in spontaneous fission of ^{252}Cf, Phys. Rev. C **9**, 632 (1974).

[107] Y. Boneh and Z. Fraenkel, Dynamic single-particle effects in fission, Phys. Rev. C **10**, 893 (1974).

[108] J. S. Pringle and F. D. Brooks, Angular correlation of neutrons from spontaneous fission of Cf^{252}, Phys. Rev. Lett. **35**, 1563 (1975).

[109] C. B. Franklyn, C. Hofmeyer, and D. W. Mingay, Angular correlation of neutrons from thermal-neutron fission of ^{235}U, Phys. Lett. B **78**, 564 (1978).

[110] C. B. Franklyn, Neutron-fragment angular correlations in ^{235}U (n_{th}, f), Radiat. Effects **92**, 323 (1986).

[111] C. Budtz-Jørgensen and H.-H. Knitter, Simultaneous investigation of fission fragments and neutrons in ^{252}Cf (SF), Nucl. Phys. **A490**, 307 (1988).

[112] B. Milek, R. Reif, and J. Revai, Model for particle emission from a fissioning system, Phys. Rev. C **37**, 1077 (1988).

[113] M. S. Samant, R. P. Anand, R. K. Choudhury, S. S. Kapoor, and D. M. Nadkarni, Prescission neutron emission in $^{235}\mathrm{U}(n_{\mathrm{th}},\mathrm{f})$ through fragment-neutron angular correlation studies, Phys. Rev. C **51**, 3127 (1995).

[114] J. K. Hwang, A. V. Ramayya, J. H. Hamilton, W. Greiner, J. D. Cole, G. M. Ter-Akopian, Yu. Ts. Oganessian, and A. V. Daniel (GANDS95 Collaboration), Search for scission neutrons in the spontaneous fission of ^{252}Cf, Phys. Rev. C **60**, 044616 (1999).

[115] N. Carjan, P. Talou, and O. Serot, Emission of scission neutrons in the sudden approximation, Nucl. Phys. **A792**, 102 (2007).

[116] R. Capote, N. Carjan, and S. Chiba, Scission neutrons for U, Pu, Cm, and Cf isotopes: Relative multiplicities calculated in the sudden limit, Phys. Rev. C **93**, 024609 (2016).

[117] I. S. Guseva, A. M. Gagarski, V. E. Sokolov, G. A. Petrov, A. S. Vorobyev, G. V. Val'sky, and T. A. Zavarukhina, Detailed investigations of neutron–neutron angular correlations in slow-neutron-induced fission of ^{233}U, ^{235}U, and ^{239}Pu, Phys. At. Nucl. **81**, 447 (2018).

[118] A. S. Vorobyev, O. A. Shcherbakov, A. M. Gagarski, G. A. Petrov, G. V. Val'ski, and T. E. Kuz'mina, Estimation of the yield of "scission" neutrons from thermal neutron-induced fission of ^{239}Pu, J. Exp. Theor. Phys. **127**, 659 (2018).